

# $(\theta_l, \theta_u)$ -Parametric Multi-Task Optimization: Joint Search in Solution and Infinite Task Spaces

Tingyang Wei, Jiao Liu, Abhishek Gupta, Puay Siew Tan, and Yew-Soon Ong, *Fellow, IEEE*

**Abstract**—Multi-task optimization is typically characterized by a fixed and finite set of optimization tasks. The present paper relaxes this condition by considering a non-fixed and potentially infinite set of optimization tasks defined in a parameterized, continuous and bounded task space. We refer to this unique problem setting as parametric multi-task optimization (PMTO). Assuming the bounds of the task parameters to be  $(\theta_l, \theta_u)$ , a novel  $(\theta_l, \theta_u)$ -PMTO algorithm is crafted to enable joint search over tasks and their solutions. This joint search is supported by two approximation models: (1) for mapping solutions to the objective spaces of all tasks, which provably accelerates convergence by acting as a conduit for inter-task knowledge transfers, and (2) for probabilistically mapping tasks to the solution space, which facilitates evolutionary exploration of under-explored regions of the task space. At the end of a full  $(\theta_l, \theta_u)$ -PMTO run, the acquired models enable rapid identification of optimized solutions for any task lying within the specified bounds. This outcome is validated on both synthetic test problems and practical case studies, with the significant real-world applicability of PMTO shown towards fast reconfiguration of robot controllers under changing task conditions. The potential of PMTO to vastly speedup the search for solutions to minimax optimization problems is also demonstrated through an example in robust engineering design.

**Index Terms**—Multi-task optimization, evolutionary algorithms, Gaussian process.

## I. INTRODUCTION

OPTIMIZATION tasks rarely exist in isolation. Multi-task optimization (MTO) has therefore emerged as a promising approach for solving problems simultaneously by leveraging shared information across related tasks [1]. This concept has been successfully applied in both evolutionary computation [2] and Bayesian optimization [3] supported by knowledge transfer strategies such as solution-based transfer [2], [4] and model-based transfer [3], [5], [6]. The applicability of these methods has been studied in a variety of domains, including robotics [7], time series prediction [8], vehicle shape design [9], and others [10], achieving faster convergence under limited computational budgets.

T. Wei and J. Liu are with the College of Computing and Data Science, Nanyang Technological University, Singapore (e-mail: TINGYANG001@e.ntu.edu.sg, jiao.liu@ntu.edu.sg)

A. Gupta is with the School of Mechanical Sciences, Indian Institute of Technology, Goa, India (e-mail: abhishekgupta@iitgoa.ac.in)

P. S. Tan is with the Singapore Institute of Manufacturing Technology (SIMTech), Agency for Science, Technology and Research, Singapore (e-mail: pstan@simtech.a-star.edu.sg)

Y.-S. Ong is with the College of Computing and Data Science, Nanyang Technological University, Singapore, and also with the Centre for Frontier AI Research (CFAR), Agency for Science, Technology and Research, Singapore (e-mail: asysong@ntu.edu.sg)

MTO is typically characterized by a fixed and finite set of optimization tasks. In this paper, we relax this paradigm by introducing parametric multi-task optimization (PMTO) as a framework that considers a non-fixed and potentially infinite set of optimization tasks within a parameterized, continuous, and bounded task space  $\Theta \subset \mathbb{R}^D$ . Each task in PMTO is defined by a unique vector  $\theta \in (\theta_l, \theta_u)$ , where  $\theta$  represents the *task parameters*. Fig. 1 illustrates the difference between MTO and PMTO. As shown in Fig. 1(a), the objective functions in MTO are defined as independent mappings from a unified decision space to task-specific objective spaces. In contrast, a task's parametrization directly influences the mapping from solutions to objectives in PMTO. This inclusion of a task space brings opportunities and challenges. PMTO benefits from leveraging information from both solution and task representations, enabling more effective inter-task relationship analysis and potentially more efficient cross-task optimization. However, continuous task parameters also imply an infinite task set, posing a challenge for algorithm development compared to the simpler case of a fixed task set in MTO.

To address PMTO problems, this paper introduces a novel  $(\theta_l, \theta_u)$ -PMTO algorithm that incorporates a joint search over solutions and tasks. The algorithm approximates the mapping  $f : \mathcal{X} \times \Theta \rightarrow \mathbb{R}$  from the solution space to the objective space by including task parameters as side information, thereby capturing correlations and facilitating the transfer of knowledge across tasks for provably faster convergence.  $(\theta_l, \theta_u)$ -PMTO also induces a probabilistic model  $\mathcal{M} : \Theta \rightarrow \mathcal{X}$  mapping tasks to their corresponding optimized solutions, with the inter-task relationships captured by the model helping support the evolutionary exploration of undersampled tasks. Through an iterative search process, the algorithm collects data on representative points that cover the task space. A well-calibrated task model  $\mathcal{M}$  obtained by the end of a  $(\theta_l, \theta_u)$ -PMTO run can then enable rapid identification of near-optimal solutions for any task in that space.

The practical implications of PMTO are particularly profound in applications that require fast adaptation in diverse and uncertain environments. Taking robotic control as an example [11], [12], standard MTO can be configured for multiple predefined morphologies of robots to achieve specific tasks including navigation, manipulation, and locomotion. However, real-world scenarios often involve unexpected changes, such as unforeseen damages or obstacles. These changes may cause the actual problem setup to deviate significantly from the predefined MTO set, leading to inferior results when obtained solutions are applied to unforeseen tasks. PMTO addresses this challenge seamlessly by optimizing over a non-fixed and

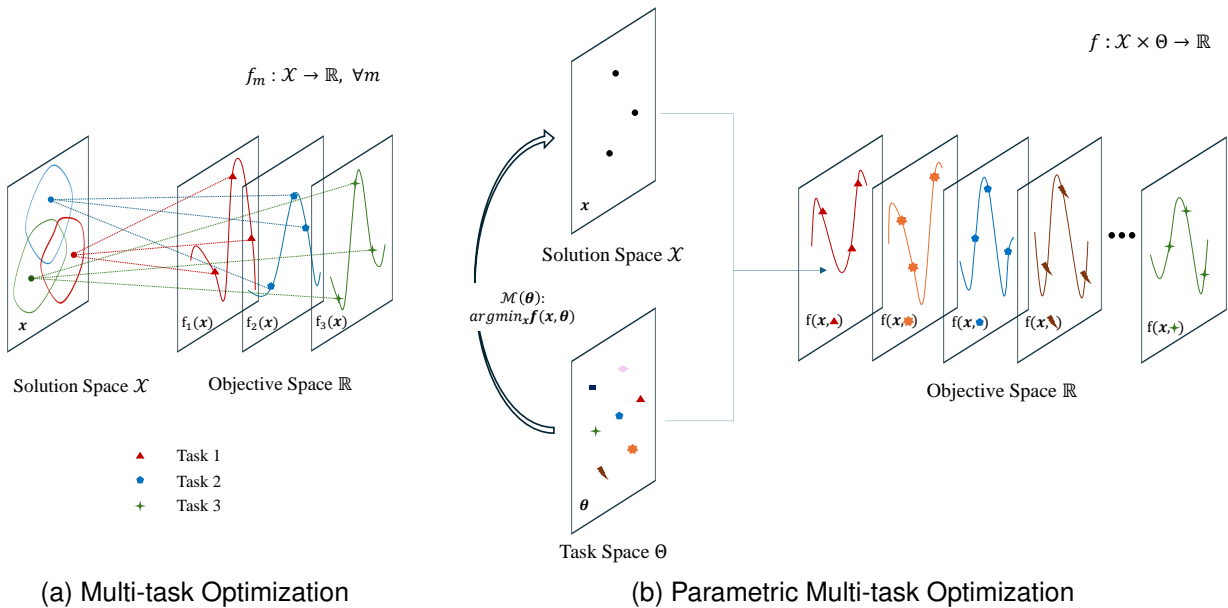


Fig. 1. Distinguishing multi-task optimization and parametric multi-task optimization. (a) In multi-task optimization, objective functions of a fixed set of tasks (3 in this example) map solutions directly to the objective space. (b) In parametric multi-task optimization, objective functions include both the solution and the task parameters  $\theta$  as arguments. Continuous task parameters imply a potentially infinite set of tasks.

potentially infinite set of tasks in advance. This approach allows the operating morphology or damage conditions to be encoded as continuous parameters within the task space, thereby enhancing the generalizability of obtained solutions to diverse problem settings.

PMTO seeks to simultaneously explore solutions for a range of parameterized tasks, making it a versatile framework for addressing problem classes where such task spaces naturally occur. Consider minimax optimization in robust engineering design [13] as an example, where the goal is to identify designs that are worst-case optimal under random variations in the design parameters. This involves optimizing (minimizing) the worst (maximum) objective value to account for real-world variabilities. By re-imagining the space of random variations as the solution space ( $\mathcal{X}$ ) and the original design parameters to form the task space ( $\Theta$ ), the robust optimization problem can be recast in the new light of PMTO. Related mathematical programs, such as bilevel programming which is known to be amenable to MTO approaches [14], can also be recast in this way. A case study demonstrating this novel application to minimax optimization is presented in Section VI-E.

In this paper, we focus on expensive optimization problems in PMTO settings. Assessing the performance of black-box optimization under stringent budget constraints is deemed especially meaningful as real-world problems frequently entail costly function evaluation calls. The major contributions of this paper are summarized below.

- We introduce the concept of PMTO as a generalization of MTO. The distinctive feature of this paradigm is the inclusion of a continuous task space, resulting in a potentially infinite number of optimization tasks within that space.
- We theoretically and empirically show that incorporating

continuous task parameters into the optimization loop enables faster convergence even when optimizing a fixed set of tasks, compared to optimizing them separately and independently.

- We propose a  $(\theta_l, \theta_u)$ -PMTO algorithm by coupling multi-task optimization in the solution space with an evolutionary algorithm (EA) for evolving tasks in the task space. The algorithm facilitates data acquisition and training of a well-calibrated task model ( $\mathcal{M}$ ) capable of predicting optimized solutions for any task parameterized by  $\theta \in (\theta_l, \theta_u)$ .
- Rigorous experimental investigation of the overall method is carried out on synthetic test problems with varied properties. The utility of the derived task model is showcased in different real-world applications spanning adaptive control systems and robust engineering design.

The remainder of this paper is organized as follows. Section II reviews related works on multitasking and parametric programming. Section III presents preliminaries including standard multi-task optimization, the parametric multi-task optimization formulation, and approximations via probabilistic Gaussian process (GP) models. Section IV discusses a restricted version of PMTO with a fixed and finite set of parameterized tasks, theoretically proving that the inclusion of task parameters accelerates convergence. Section V introduces our novel algorithm, dubbed  $(\theta_l, \theta_u)$ -PMTO, for jointly searching over both solution and task spaces. Section VI empirically verifies the effectiveness of the method on a variety of synthetic and practical problems, establishing PMTO as a promising direction for future research. Section VII concludes the paper.

## II. RELATED WORKS

### A. Multi-task Optimization

In black-box optimization, MTO deals with a fixed set of tasks simultaneously within limited evaluation budgets. In the Bayesian optimization literature, MTO usually leverages GPs with multi-task kernels [3], modeling both data inputs and task indices to capture inter-task relationships. A multi-task GP [15] is equipped to transfer information from related source tasks to enhance model performance in a target task, with associated multi-task Bayesian optimization algorithms demonstrating their effectiveness in both unconstrained [16] and constrained optimization settings [17].

In evolutionary computation, multitasking [2], [18] has proven to be effective for high-dimensional [1], [4], [19], [20] and combinatorial optimization problems [21]–[23]. Leveraging the implicit parallelism of evolutionary algorithms [1], [2], evolutionary multi-task optimization facilitates knowledge transfer by either implicitly sharing high-quality solutions across optimization tasks [2], [24] or explicitly mapping solutions from source domains to target domains [5], [6]. In solution-based transfer, the solution distribution of a source task may be shifted according to handcrafted translation vectors [25], [26] or the multi-task search may be guided by the maximum point of the product of population distributions of a source-target task pair [27]. In model-based knowledge transfer, a pair-wise mapping from a source to the target task is established by distinct learning-based methods including least square methods [5], [6], subspace alignment [28], manifold alignment [29], geodesic flow [30], among others [31], [32]. Building on these knowledge transfer strategies, evolutionary multi-task optimization has shown promise across a plethora of applications [10], including job shop scheduling [33], sparse reconstruction [34], point cloud registration [35], and recommender systems [36].

Despite considerable research efforts, existing methods primarily focus on traditional MTO problems with a fixed and finite set of optimization tasks, without considering parameterizations of the tasks themselves. Recent work on parametric-task MAP-Elites [37] fills this gap to some extent, but is limited by an exhaustive black-box algorithm that precludes application to real-world problems with tight evaluation budgets. In contrast, the notion of PMTO introduced in this paper not only caters to infinite task sets by jointly searching over continuous solution and task spaces but also emphasizes data-efficiency in expensive optimization domains.

### B. Parametric Programming

Parametric programming is a type of mathematical optimization framework that seeks to derive optimal solutions as a function of uncertain (task) parameters [38]. Associated techniques have been applied in diverse optimization contexts including linear programming [39], mixed integer programming [40], or nonlinear programming [38], [41]. Generally coupled with model predictive control frameworks [42], parametric programming has shown promising results in adaptive control systems encompassing energy management of hybrid vehicles [43], autonomous steering control [44], current

control in power electronics [45], and endoscope control in biomedical cases [46], among others [38]. Being an active but nascent area of research, parametric programming techniques typically limit to problems that possess a precise mathematical description, thus precluding application to problems that involve expensive, black-box objective functions. Our proposed  $(\theta_l, \theta_u)$ -PMTO algorithm addresses this gap by inducing computationally cheap approximations in a joint exploration of solution and parametrized task spaces, thereby distinguishing from any related work in the literature.

## III. PRELIMINARIES

### A. Multi-task Optimization

Standard MTO aims to simultaneously solve  $M$  optimization tasks,  $\mathcal{T}_1, \mathcal{T}_2, \dots, \mathcal{T}_M$ . The group of tasks can be formulated as follows:

$$\operatorname{argmin}_{\mathbf{x}_m \in \mathcal{X}_m} f_m(\mathbf{x}_m), \quad m \in [M], \quad (1)$$

where the decision vector  $\mathbf{x}_m$  of the  $m$ -th optimization task lies in search space  $\mathcal{X}_m$  and optimizes the objective function  $f_m : \mathcal{X}_m \rightarrow \mathbb{R}$  [2]. It is commonly assumed in black-box MTO that no prior knowledge or side information about the tasks is available. As a result, evolutionary or Bayesian MTO algorithms must adaptively identify task similarities or correlations during the optimization process to enhance convergence and mitigate the risk of negative transfer [1], [4].

### B. Parametric Multi-task Optimization

PMTO contains additional task parameters as side information, leading to the following formulation:

$$\operatorname{argmin}_{\mathbf{x} \in \mathcal{X}} f(\mathbf{x}, \boldsymbol{\theta}), \quad \forall \boldsymbol{\theta} \in \Theta, \quad (2)$$

where  $\Theta \subset \mathbb{R}^D$  is a bounded continuous space such that each optimization task is represented by a unique parameter vector  $\boldsymbol{\theta} \in \Theta$ . Comparing (2) to the formulation (1), two major differences between MTO and PMTO surface.

- The MTO problem does not assume any prior knowledge or side information about the constitutive optimization tasks. In contrast, PMTO assumes side information in the form of task parameters to be available and usable in the optimization loop.
- MTO limits the search process within the solution spaces  $\{\mathcal{X}_m\}_{m=1}^M$  of a fixed set of optimization tasks  $\{\mathcal{T}_m\}_{m=1}^M$ . PMTO generalizes this idea by considering a task space containing potentially infinite tasks characterized by continuous task parameters, i.e.,  $\forall \boldsymbol{\theta} \in \Theta$ .

If we consider the problem in (2) to be solved for a representative set of tasks in  $\Theta$ , a task model  $\mathcal{M} : \Theta \rightarrow \mathcal{X}$  could then be induced to map tasks to their corresponding optimized solutions in  $\mathcal{X}$ . Through effective generalization, the model would then enable rapid generation of solutions for any task in  $\Theta$ . Specifically, the task model is constructed to approximate solutions to (2) as:

$$\forall \boldsymbol{\theta} \in \Theta, \quad \mathcal{M}(\boldsymbol{\theta}) = \operatorname{argmin}_{\mathbf{x} \in \mathcal{X}} f(\mathbf{x}, \boldsymbol{\theta}). \quad (3)$$

---

**Algorithm 1:** GP-based Optimization

---

**Data:** Initialization budgets  $N_{init}$ , Total evaluation budgets  $N_{tot}$ , Objective function  $f$ ;  
**Result:** The best solution found in solution set  $\mathcal{D}$ ;

- 1 Randomly initialize  $N_{init}$  solutions  $\{\mathbf{x}^{(i)}\}_{i=1}^{N_{init}}$
- 2 Evaluate initial solutions via the objective function  $f(\cdot)$
- 3  $\mathcal{D} \leftarrow \{(\mathbf{x}^{(i)}, f(\mathbf{x}^{(i)}))\}_{i=1}^{N_{init}}$
- 4  $t \leftarrow 0$
- 5 Train the GP model on  $\mathcal{D}$
- 6 **while**  $t + N_{init} < N_{tot}$  **do**
- 7     Sample new input data  $\mathbf{x}^{(t)}$  based on (6)
- 8      $\mathcal{D} \leftarrow \mathcal{D} \cup \{(\mathbf{x}^{(t)}, f(\mathbf{x}^{(t)}))\}$
- 9     Update the GP model according to  $\mathcal{D}$
- 10     $t \leftarrow t + 1$
- 11 **end**

---

C. Gaussian Process

Throughout the paper, GP models [47] are adopted for principled probabilistic function approximation. Given an unknown function  $f$ , the GP assumes  $f$  to be a sample of a Gaussian prior, i.e.,  $f \sim \mathcal{GP}(\mu(\cdot), \kappa(\cdot, \cdot))$ , defined by the mean function  $\mu(\mathbf{x}) = \mathbb{E}[f(\mathbf{x})]$  and the covariance function  $\kappa(\mathbf{x}, \mathbf{x}') = Cov[f(\mathbf{x}), f(\mathbf{x}')]$ . Given a dataset  $\mathcal{D} = \{(\mathbf{x}^{(i)}, y^{(i)})\}_{i=1}^N$ , where  $y^{(i)} = f(\mathbf{x}^{(i)}) + \epsilon^{(i)}$  and  $\epsilon^{(i)} \sim \mathcal{N}(0, \sigma_\epsilon^2)$ , the predicted posterior distribution of the GP, i.e.,  $\mathcal{N}(\mu(\mathbf{x}), \sigma^2(\mathbf{x}))$ , at an unseen query point  $\mathbf{x}$  can be computed as:

$$\mu(\mathbf{x}) = \mathbf{k}^\top (\mathbf{K} + \sigma_\epsilon^2 \mathbf{I}_N)^{-1} \mathbf{y}, \quad (4)$$

$$\sigma(\mathbf{x}) = \kappa(\mathbf{x}, \mathbf{x}) - \mathbf{k}^\top (\mathbf{K} + \sigma_\epsilon^2 \mathbf{I}_N)^{-1} \mathbf{k}, \quad (5)$$

where  $\mathbf{k}$  is the kernel vector between  $\mathbf{x}$  and the data in  $\mathcal{D}$ ,  $\mathbf{K}$  is an  $N \times N$  matrix with elements  $\mathbf{K}_{p,q} = \kappa(\mathbf{x}^{(p)}, \mathbf{x}^{(q)})$ ,  $p, q \in \{1, \dots, N\}$ ,  $\mathbf{I}_N$  is a  $N \times N$  identity matrix, and  $\mathbf{y}$  is the vector of noisy observations of the output function of interest.

A GP-based optimization pipeline leverages the uncertainty quantification capabilities of GPs to balance the exploitation and exploration of search spaces under black-box objective functions [48], making it widely applicable across a plethora of real-world optimization problems [49], [50]. A pseudo-code for GP-based optimization is provided in **Algorithm 1**. This optimization process proceeds iteratively, with each iteration generating a query solution using an acquisition function. The procedure for obtaining the query solution in the  $t$ -th iteration can be expressed as:

$$\mathbf{x}^{(t)} = \operatorname{argmax}_{\mathbf{x} \in \mathcal{X}} \alpha(\mathbf{x}; \{(\mathbf{x}_i, f(\mathbf{x}_i))\}_{i=1}^{t+N_{init}}), \quad (6)$$

where  $\alpha(\cdot)$  denotes the acquisition function. Many acquisition functions have been studied over the years including the expected improvement [51], upper confidence bound (UCB) [48], knowledge gradient [52], or entropy search [53].

IV. PARAMETRIC MULTI-TASK OPTIMIZATION WITH A FIXED TASK SET

In this section, we prove that incorporating the task parameter  $\theta$  into the optimization process enhances convergence

rates in PMTO. For simplicity, we focus on a restricted version of the PMTO problem, considering only a finite and fixed set of optimization tasks  $\{\mathcal{T}_m\}_{m=1}^M$  parameterized by  $\{\theta_m\}_{m=1}^M$ . Since we consider solving optimization problems under limited evaluation budgets, the GP-based optimization in **Algorithm 1** serves as an established baseline method. All subsequent analysis and discussions are therefore grounded in the framework of GP-based optimization.

A. Optimization of Fixed Parameterized Tasks

As an instantiation of **Algorithm 1**, we employ the well-studied UCB<sup>1</sup> [48] acquisition function, defined as follows:

$$\mathbf{x}^{(t)} = \operatorname{argmax}_{\mathbf{x} \in \mathcal{X}} -\mu(\mathbf{x}) + \beta \cdot \sigma(\mathbf{x}), \quad (7)$$

where the query solution  $\mathbf{x}^{(t)}$  strikes a balance between exploitation and exploration in accordance with the trade-off coefficient  $\beta$ . The methodology is further extended to the PMTO framework with fixed tasks (termed as PMTO-FT), as illustrated in **Algorithm 2**. Unlike common GP-based optimization, unified GP models are built in PMTO-FT using an augmented dataset  $\mathcal{D}_{pmt} = \cup_{m=1}^M \{(\mathbf{x}_m^{(i)}, \theta_m, f(\mathbf{x}_m^{(i)}, \theta_m))\}_{i=1}^{N_m}$ , where  $N_m$  represents the number of samples evaluated for the  $m$ -th problem. This dataset encompasses not only the evaluated solutions and their corresponding objective function values but also the task parameters  $\{\theta_m\}_{m=1}^M$ . The unified GP is thus trained to infer how a point in the product space  $\mathcal{X} \times \Theta$  maps to the objective space. Accordingly, the UCB acquisition function in PMTO-FT is defined as:

$$\mathbf{x}_m^{(t)} = \operatorname{argmax}_{\mathbf{x} \in \mathcal{X}} -\mu_{pmt}(\mathbf{x}, \theta_m) + \beta \cdot \sigma_{pmt}(\mathbf{x}, \theta_m). \quad (8)$$

Here  $\mu_{pmt}(\mathbf{x}, \theta_m)$  and  $\sigma_{pmt}(\mathbf{x}, \theta_m)$  are calculated as follows:

$$\mu_{pmt}(\mathbf{x}, \theta_m) = \mathbf{k}_{pmt}^\top (\mathbf{K}_{pmt} + \sigma_\epsilon^2 \mathbf{I}_{N_{pmt}}^{-1}) \mathbf{y}_{pmt}, \quad (9)$$

$$\sigma_{pmt}(\mathbf{x}, \theta_m) = \kappa_{pmt,*} - \tilde{\mathbf{k}}_{pmt}^\top (\mathbf{K}_{pmt} + \sigma_\epsilon^2 \mathbf{I}_{N_{pmt}})^{-1} \mathbf{k}_{pmt}, \quad (10)$$

where  $\kappa_{pmt,*} = \kappa_{pmt}((\mathbf{x}, \theta_m), (\mathbf{x}, \theta_m))$ ,  $\kappa_{pmt}(\cdot, \cdot)$  is the unified kernel function,  $\mathbf{k}_{pmt}$  is the kernel vector between  $(\mathbf{x}, \theta_m)$  and the data in  $\mathcal{D}_{pmt}$ ,  $\mathbf{K}_{pmt}$  is the kernel matrix of the data in  $\mathcal{D}_{pmt}$ ,  $\mathbf{I}_{N_{pmt}}$  is an  $N_{pmt} \times N_{pmt}$  identity matrix,  $N_{pmt}$  is the size of  $\mathcal{D}_{pmt}$ , and  $\mathbf{y}_{pmt}$  is the vector of noisy observations of the objective function values in  $\mathcal{D}_{pmt}$ . Next, we prove that the approach in **Algorithm 2**, which leverages the unified GP as a conduit for knowledge transfer between tasks, supports faster convergence than independently running **Algorithm 1** for each optimization task.

B. Theoretical Analysis

Extending the analysis technique in [48], we define the *instantaneous regret* of the  $m$ -th optimization task at the  $t$ -th evaluation as:

$$r_m(t) = f_m(\mathbf{x}_m^{(t)}) - f_m(\mathbf{x}_m^*) \geq 0, \forall m \in [M], \quad (11)$$

<sup>1</sup>The formulation is given to solve a black-box maximization problem but can also be adapted to the minimization problem by negation.

---

**Algorithm 2: PMTO-FT**


---

**Data:** Initialization budget  $N_{init}$ , Total evaluation budgets  $N_{tot}$ , Objective function  $f(\mathbf{x}, \boldsymbol{\theta})$ , Target optimization tasks  $\{\mathcal{T}_m\}_{m=1}^M$ , and corresponding task parameters  $\{\boldsymbol{\theta}_m\}_{m=1}^M$ ;

**Result:** The best solution found in solution set  $\mathcal{D}_{pmt}$  for each optimization task;

- 1  $\mathcal{D}_{pmt} \leftarrow \emptyset$
- 2 **foreach** task  $\mathcal{T}_m$  **do**
- 3     Randomly initialize  $N_{init}/M$  solutions
- 4     Evaluate the initial solutions via the parameterized objective function  $f(\cdot, \boldsymbol{\theta}_m)$  of task  $\mathcal{T}_m$
- 5      $\mathcal{D}_{pmt} \leftarrow \mathcal{D}_{pmt} \cup \{(\mathbf{x}_m^{(i)}, \boldsymbol{\theta}_m, f(\mathbf{x}_m^{(i)}, \boldsymbol{\theta}_m))\}_{i=1}^{N_{init}/M}$
- 6 **end**
- 7  $t \leftarrow 0$
- 8 Train a unified GP model on  $\mathcal{D}_{pmt}$
- 9 **while**  $t + N_{init} < N_{tot}$  **do**
- 10    **foreach** task  $\mathcal{T}_m$  **do**
- 11     Sample new input data  $\mathbf{x}_{m,q}^{(t)}$  for the current optimization task based on (8)
- 12      $\mathcal{D}_{pmt} \leftarrow \mathcal{D}_{pmt} \cup \{(\mathbf{x}_m^{(t)}, \boldsymbol{\theta}_m, f(\mathbf{x}_m^{(t)}, \boldsymbol{\theta}_m))\}$
- 13      $t \leftarrow t + 1$
- 14    **end**
- 15    Update the GP model according to  $\mathcal{D}_{pmt}$
- 16 **end**

---

where  $f_m(\cdot) = f(\cdot, \boldsymbol{\theta}_m)$  and  $\mathbf{x}_m^* = \operatorname{argmin}_{\mathbf{x} \in \mathcal{X}} f_m(\mathbf{x})$ . Thereafter, the *cumulative regret* of the  $m$ -th task over  $T$  evaluations can be defined as:

$$R_m(T) = \sum_{t=1}^T r_m(t), \forall m \in [M]. \quad (12)$$

Based on these definitions, a statistical bound on the cumulative regret for GP-based optimization procedures can be derived. This result holds under assumptions of a correctly specified GP prior, known additive noise variance  $\sigma_\epsilon^2$ , global optimization of the UCB acquisition function to ascertain  $\mathbf{x}_m^{(t)}$ , and a finite decision space  $\mathcal{X}$ . According to [48], we have,

$$\Pr\{R_m(T) \leq \sqrt{C_1 T \beta_T \gamma_{T,m}} \forall T \geq 1\} \geq 1 - \delta, \quad (13)$$

where  $C_1 = 8/\log(1 + \sigma_\epsilon^{-2})$ ,  $\beta_T$  is a predefined UCB coefficient dependent on the confidence parameter  $\delta \in [0, 1]$ ;  $\gamma_{T,m}$  is the maximal information gain (MIG) quantifying the maximal uncertainty reduction about the objective function  $f_m$  from observing  $T$  samples, which can be denoted as follows:

$$\gamma_{T,m} = \max_{\mathbf{x}_m^{(1)}, \dots, \mathbf{x}_m^{(T)}} I([y_m^{(1)}, \dots, y_m^{(T)}]; \mathbf{f}_m | \mathcal{D}_{pmt}). \quad (14)$$

Here  $\mathbf{x}_m^{(1)}, \dots, \mathbf{x}_m^{(T)}$  are the samples corresponding to the  $m$ -th task,  $\mathbf{f}_m = [f_m(\mathbf{x}_m^{(1)}), \dots, f_m(\mathbf{x}_m^{(T)})]$ ,  $[y_m^{(1)}, \dots, y_m^{(T)}]$  are the observed noisy outputs, and  $I$  represents the mutual information between  $\mathbf{f}_m$  and  $[y_m^{(1)}, \dots, y_m^{(T)}]$ . From (13), we see that the cumulative regret bound is determined primarily by the MIG. Thus, comparing the MIG under PMTO-FT with that for separately and independently solved tasks shall translate to

a theoretical comparison of their respective convergence rates. A lower MIG implies tighter regret bounds and hence suggests faster convergence. Denoting the MIG of the independent strategy as  $\gamma_{T,m}^{ind}$ , we establish the following theorem.

**Theorem.** *Let the kernel functions used in PMTO-FT and the independent strategy satisfy  $\kappa_{pmt}((\mathbf{x}, \boldsymbol{\theta}), (\mathbf{x}', \boldsymbol{\theta})) = \kappa_{ind}(\mathbf{x}, \mathbf{x}')$ . Then, the MIG in the independent strategy, denoted as  $\gamma_{T,m}^{ind}$ , and the MIG in the PMTO-FT, denoted as  $\gamma_{T,m}$ , satisfy  $\gamma_{T,m} \leq \gamma_{T,m}^{ind}, \forall m \in [M], \forall T \geq 1$ .*

**Remark 1.** *Given an evaluation budget of  $(M \times T)$ , each objective function  $f_m(\cdot), \forall m \in [M]$ , is evaluated  $T$  times in both PMTO-FT and the independent GP-based optimization procedure. This ensures a fair distribution of the computational budget across tasks while comparing the cumulative regret bounds of the two algorithms.*

A detailed proof is in the appendix. According to the result, incorporating task parameters  $\{\boldsymbol{\theta}_m\}_{m=1}^M$  as side information results in a lower MIG for the PMTO-FT method compared to the independent strategy. This translates to faster convergence in PMTO-FT relative to its single-task counterpart. Furthermore, due to the explicit modeling of inter-task relationships through the unified GP kernel, PMTO-FT's approximation model can potentially generalize to tasks beyond the fixed training set of  $M$  optimization tasks. This attribute positions PMTO-FT as a promising approach for extension to address the problem defined by formulations (2) and (3).

## V. THE $(\boldsymbol{\theta}_l, \boldsymbol{\theta}_u)$ -PMTO ALGORITHM

In this section, we present the  $(\boldsymbol{\theta}_l, \boldsymbol{\theta}_u)$ -PMTO algorithm that relaxes PMTO-FT's constraint of a fixed task set. The proposed method integrates a probabilistic task model that fulfills two key roles. First, it learns to predict optimized solutions for parameterized tasks within the continuous and bounded task space, thereby broadening optimization capacity from a fixed set to the entire task space. Second, the inter-task relationships captured by the model help guide an evolutionary search over under-explored regions of the task space—a process termed *task evolution*—supporting the acquisition of informative data that enhances the performance of the approximation models.

### A. Overview of the $(\boldsymbol{\theta}_l, \boldsymbol{\theta}_u)$ -PMTO

A pseudocode of the proposed  $(\boldsymbol{\theta}_l, \boldsymbol{\theta}_u)$ -PMTO is detailed in **Algorithm 3** and its key steps are explained below.

- **Initialization:**  $M$  parameterized optimization tasks are initiated by randomly sampling a set of task parameters  $\Psi = \{\boldsymbol{\theta}_m\}_{m=1}^M$  in the task space.  $N_{init}/M$  solutions are initialized and evaluated for each task, to form dataset  $\mathcal{D}_{pmt}$ . A dataset  $\mathcal{D}^*$ , which includes only the current best evaluated samples corresponding to all task parameters in  $\Psi$ , is also induced.
- **Approximation Models:** In steps **9** to **10** and steps **21** to **23**, a unified GP model (with inputs comprising both the solutions and the task parameters) and a task model  $\mathcal{M}$  are built based on dataset  $\mathcal{D}_{pmt}$  and  $\mathcal{D}^*$ , respectively. The unified GP approximates the mapping from the product

---

**Algorithm 3:**  $(\theta_l, \theta_u)$ -PMTO

---

**Data:** Initial task size  $M$ , Initialization budget  $N_{init}$ , Total budgets for each task  $N_{tot}$ , Objective function  $f(\mathbf{x}, \theta)$ , Evaluated solution set  $\mathcal{D}_{pmt}$ , Task pool  $\Psi$ ;

**Result:** Best solution found for each optimization task;

- 1  $\mathcal{D}_{pmt} \leftarrow \emptyset$
- 2  $\Psi \leftarrow \{\theta_m\}_{m=1}^M$
- 3 **foreach** task parameter in  $\Psi$  **do**
- 4     Randomly initialize  $N_{init}/M$  solutions
- 5     Evaluate the objective function for the initial solutions via  $f(\cdot, \theta_m)$
- 6      $\mathcal{D}_{pmt} \leftarrow \mathcal{D}_{pmt} \cup \{(\mathbf{x}_m^{(i)}, \theta_m, f(\mathbf{x}_m^{(i)}, \theta_m))\}_{i=1}^{N_{init}/M}$
- 7 **end**
- 8 Let  $\mathbf{x}_m^*$  be the current best solution corresponding to the optimization task parameterized by  $\theta_m$ , then  $\mathcal{D}^* \leftarrow \{(\theta_m, \mathbf{x}_m^*)\}_{m=1}^M$
- 9 Train a unified GP model on  $\mathcal{D}_{pmt}$
- 10 Train the task model  $\mathcal{M}$  on  $\mathcal{D}^*$
- 11  $t \leftarrow 0$
- 12 **while**  $t + N_{init} < N_{tot}$  **do**
- 13      $\theta_{new} \leftarrow \text{Task-Evolution}(\mathcal{M}, \Psi, P, G)$
- 14      $\Psi \leftarrow \Psi \cup \{\theta_{new}\}$
- 15      $M \leftarrow M + 1$
- 16     **foreach** task parameter  $\theta_m$  in  $\Psi$  **do**
- 17         Sample new input data  $\mathbf{x}_m^{(t)}$  for the current optimization task based on (8)
- 18          $\mathcal{D}_{pmt} \leftarrow \mathcal{D}_{pmt} \cup \{(\mathbf{x}_m^{(t)}, \theta_m, f_m(\mathbf{x}_m^{(t)}, \theta_m))\}$
- 19          $t \leftarrow t + 1$
- 20     **end**
- 21     Update the unified GP model on  $\mathcal{D}_{pmt}$
- 22     Let  $\mathbf{x}_m^*$  be the current best solution corresponding to the  $m$ -th task parameters in  $\Psi$ , then  $\mathcal{D}^* \leftarrow \{(\theta_m, \mathbf{x}_m^*)\}_{m=1}^M$
- 23     Update the task model  $\mathcal{M}$  on  $\mathcal{D}^*$
- 24 **end**

---

space  $\mathcal{X} \times \Theta$  to the objective space, while the task model maps points in the task space  $\Theta$  to their corresponding elite solutions.

- *Task Evolution:* In steps 13 to 14, the inter-task relationships captured by the task model  $\mathcal{M}$  are used to guide an EA to search for new tasks to be included in the task pool  $\Psi$ . The details of the task evolution module can be found in Section V-C.
- *Cross-task Optimization:* In lines 16 to 20, the predictive distribution of the unified GP is used to define acquisition functions, formulated in (8), whose optimization yield high-quality solutions for each task in  $\Psi$ .

At the end of a full  $(\theta_l, \theta_u)$ -PMTO run, the algorithm returns the best solutions found for each task in the pool  $\Psi$ , and the resultant task model  $\mathcal{M}$ .

---

**Algorithm 4:** Task Evolution

---

**Data:** Task pool  $\Psi$ , Task model  $\mathcal{M}$ , Population size  $P$ , Maximum generations  $G$ ;

**Result:** New task parameter  $\theta_{new}$ ;

- 1 Initialize a population  $\{\theta_0^{(p)}\}_{p=1}^P$  of candidate task parameters
- 2 Evaluate scores  $g(\theta_0^{(p)})$  using equation (17)
- 3 **for**  $\tau = 1$  **to**  $G$  **do**
- 4     Select parents using binary tournament selection
- 5     Generate offspring with SBX crossover
- 6     Apply PM to mutate offspring
- 7     Evaluate  $g(\theta)$  for offspring individuals; Combine parent and offspring populations
- 8     Select top  $P$  individuals as  $\{\theta_\tau^{(p)}\}_{p=1}^P$  based on  $g(\theta)$  scores;
- 9 **end**
- 10 Return  $\theta_{new} = \operatorname{argmax}_{\theta \in \{\theta_G^{(p)}\}_{p=1}^P} g(\theta)$

---

### B. GP-based Task Model

The dataset  $\mathcal{D}^* = \{(\theta_m, \mathbf{x}_m^*)\}_{m=1}^M$ , where  $\mathbf{x}_m^*$  indicates the best solution found so far for parametrized task  $\theta_m$ , can be used to approximate a mapping from tasks to their optimized solutions. We instantiate this task model by concatenating multiple independent GPs. Specifically, assuming  $\mathcal{X} \subset \mathbb{R}^V$ ,  $V$  GPs are built with each model corresponding to a separate dimension of the solution space. For the  $v$ -th dimension, a data subset is constructed as  $\mathcal{D}_v^* := \{(\theta_m, \mathbf{x}_{m,v}^*)\}_{m=1}^M$ . Given  $\mathcal{D}_v^*$ , the posterior estimate of the  $v$ -th decision variable value,  $\mathcal{M}_v(\theta) = \mathcal{N}(\tilde{\mu}_v(\theta), \tilde{\sigma}_v(\theta))$ , for a queried optimization task  $\theta$  is given as:

$$\tilde{\mu}_v(\theta) = \tilde{\mathbf{k}}_v^\top (\tilde{\mathbf{K}}_v + \sigma_{\epsilon,v}^2 \mathbf{I}_M)^{-1} \mathbf{x}_v, \quad (15)$$

$$\tilde{\sigma}_v(\theta) = \tilde{\kappa}_v(\theta, \theta) - \tilde{\mathbf{k}}_v^\top (\tilde{\mathbf{K}}_v + \sigma_{\epsilon,v}^2 \mathbf{I}_M)^{-1} \tilde{\mathbf{k}}_v, \quad (16)$$

where  $\tilde{\kappa}_v(\cdot, \cdot)$  is the kernel function used in the  $v$ -th model,  $\tilde{\mathbf{k}}_v$  denotes the kernel vector between parameters of the queried task and the existing task parameters in  $\Psi$ ,  $\tilde{\mathbf{K}}_v$  is the overall kernel matrix of the  $v$ -th GP,  $\mathbf{x}_v$  is a column vector containing the  $v$ -th variable of all solutions in dataset  $\mathcal{D}_v^*$ , and  $\sigma_{\epsilon,v}$  is the noise term of the  $v$ -th GP. The concatenated output of the task model is then given as  $\mathcal{M}(\theta) = [\mathcal{M}_1(\theta), \dots, \mathcal{M}_V(\theta)]^T$ , such that  $\mathcal{M}(\theta)$  lies in the solution space  $\mathcal{X} \subset \mathbb{R}^V$ .

### C. Task Evolution

The effectiveness of the GP-based task model depends on the coverage of the sampled task parameters (with greater density in regions where the mapping from task to solution space may be complex), making the sampling process crucial for better model calibration and prediction of optimal solutions for unseen tasks. To address this, a task evolution module in  $(\theta_l, \theta_u)$ -PMTO actively searches under-explored regions of the task space during optimization. A direct comparison of task evolution versus the random sampling of tasks is presented in the numerical studies.



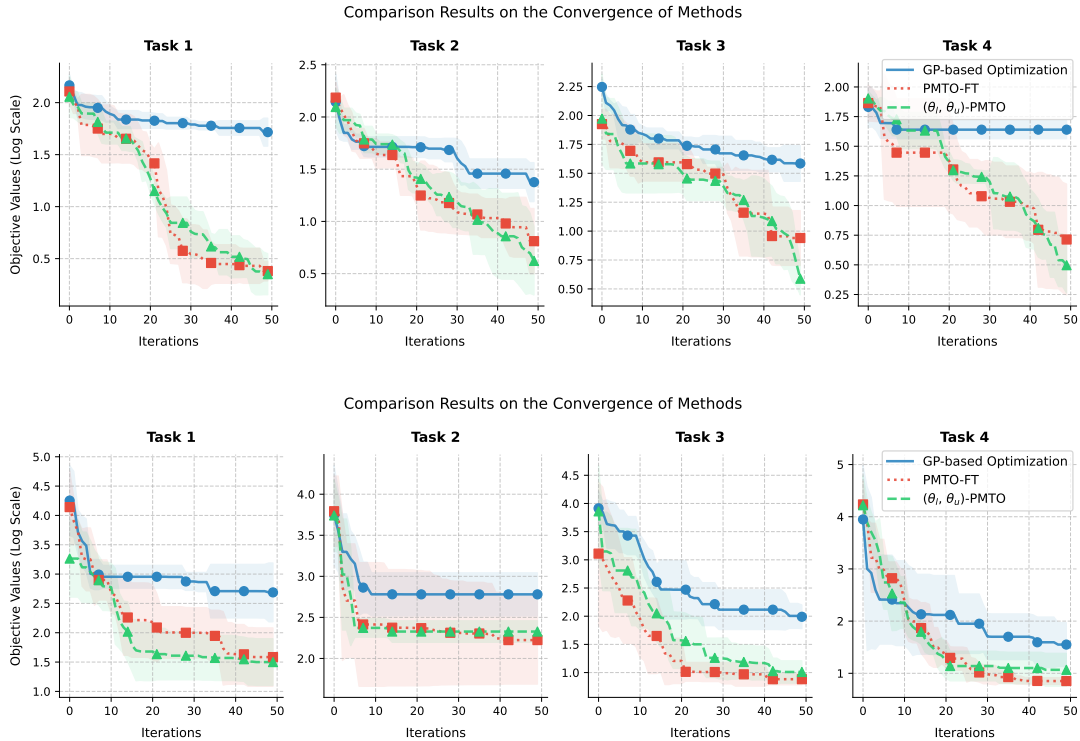


Fig. 2. Convergence trends of optimization methods for Ackley-II (top) and Griewank-II (bottom) on four sample tasks each.

To build a well-calibrated task model, it is essential to sample diverse tasks, ensuring a good coverage of the task space. This is accomplished by searching for  $\theta$  that optimizes the following objective function:

$$g(\theta) = \sum_{v=1}^V \det Q_v([\theta_1, \theta_2, \dots, \theta_M, \theta]), \quad (17)$$

where  $Q_v$  is a  $(M+1) \times (M+1)$  matrix with element  $Q_{v,i,j} = \tilde{\kappa}_v(\theta_i, \theta_j)$ , and  $\theta_i, \theta_j \in \{\theta_m\}_{m=1}^M \cup \{\theta\}$ . The  $(i, j)$ -th element of the matrix thus captures the inter-task relationship between task pair  $\theta_i$  and  $\theta_j$  as defined by the  $v$ -th kernel function. The overall objective function essentially prioritizes those unseen tasks for which the GP-based task model depicts high predictive uncertainty. From a geometric perspective, the determinant of the matrix  $Q_v$  represents the volume of a parallelepiped spanned by feature maps constructed by the kernel function  $\tilde{\kappa}_v$  [54], [55]. Taking the average over each dimension of the solution space, it is expected that evolved tasks  $\theta_{new} = \operatorname{argmax}_{\theta \in \Theta} g(\theta)$  shall enable a diversity-aware search in the task space and hence facilitate the search for under-explored regions of that space.

To optimize the objective function  $g(\theta)$  in each iteration of  $(\theta_l, \theta_u)$ -PMTO, we adopt the simple EA described in **Algorithm 4**. The EA incorporates polynomial mutation (PM) [56] and simulated binary crossover (SBX) [57]. Binary tournament selection is employed to impart selection pressure for evolving tasks from one generation to the next.

## VI. RESULTS

### A. Experimental Settings

In this section, we assess the effectiveness of the proposed  $(\theta_l, \theta_u)$ -PMTO on various PMTO problems, encompassing

synthetic problems, three adaptive control problems, and a robust engineering design problem. We compare  $(\theta_l, \theta_u)$ -PMTO to GP-based optimization introduced in **Algorithm 1** and PMTO-FT introduced in **Algorithm 2**. All algorithms employ the UCB as the acquisition function, with  $\beta$  set to 1.0 in (7) and (8). Across all problems, the total evaluation budget  $N_{tot}$  is 2000 and the initialization budget  $N_{init}$  is 200. For GP-based optimization and PMTO-FT, the target optimization tasks are randomly sampled in the task space via Latin hypercube sampling [58] with the sample size  $M$  of 20. The GP models applied in all the methods are configured with the same hyperparameters. To optimize the hyperparameters of the GP, the Adam optimizer [59] with a learning rate of 0.01 and a maximum epoch of 500 is employed. For the task evolution module, P and G are set to 100 and 50, respectively, the SBX crossover operator is parameterized by distribution index  $\eta_c = 15$  and  $p_c = 0.9$ , and the PM mutation operator is parameterized by distribution index  $\eta_m = 20$  and  $p_m = 0.9$ .

### B. Performance Metrics

To assess the performance of the proposed method, we conduct  $U = 20$  independent trials of experiments for each algorithm, and numbers with indicators (+), (−) and ( $\approx$ ) imply that the compared algorithm is better than, worse than, or similar to the proposed  $(\theta_l, \theta_u)$ -PMTO at 90% confidence level as per the Wilcoxon signed-rank test. Since GP-based optimization and PMTO-FT lack task models capable of addressing infinite parameterized tasks, for fairness, task models are constructed offline for these two algorithms as part of the evaluation process. Per trial, optimization results produced by GP-based

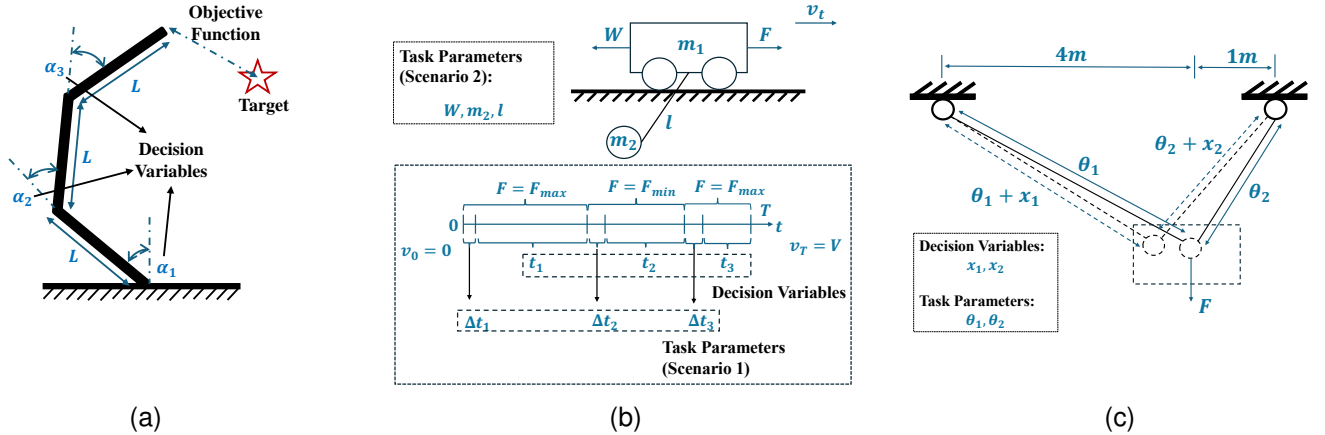


Fig. 3. The illustrative examples for the case studies: (a) Parametric Robot Arm Optimization: Optimize the angular position of each joint ( $\alpha_1, \alpha_2, \alpha_3$ ) so that the end effector can approach as close as to the target position. Task parameters include the length of each arm  $L$  and the maximum rotation degree  $\alpha_{max}$ . (b) Parametric Crane-Load System Optimization: Optimize the time intervals  $t_1, t_2, t_3$  during which the distinct drive forces  $F$  are exerted on the crane-load system so that the system can achieve a goal velocity with minimal operating time and oscillation. Task parameters include Scenario 1: time delays  $\Delta t_1, \Delta t_2, \Delta t_3$ , and Scenario 2: operating conditions including the length of suspension  $l$ , the mass of load  $m_2$ , and the resistance  $W$ . (c) Plane Truss Design: Optimize the lengths of two bars  $\theta_1, \theta_2$  to minimize the overall structural weight and the joint displacement in aware of possible processing errors  $x_1, x_2$ . The exact formulation of the (b) and (c) can be found in the supplementary materials.

optimization and PMTO-FT are collected first, and then the task models are built based on (15) and (16). For evaluation, a set of randomly sampled task parameters is provided to the task model, which then generates a set of predicted solutions accordingly. These solutions are subsequently evaluated via the objective function and ranked based on their objective values. Quantiles are recorded at the 5th, 25th, 50th, 75th, and 95th percentiles to assess solution quality across sampled tasks. The mean value for each quantile is then computed across all trials to evaluate the performance distribution.

To define the evaluation metrics, let the set of sampled task parameters be  $\bar{\Theta} = \{\theta_1, \theta_2, \dots, \theta_K\}$ . For each trial  $u \in [U]$ , the task model  $\mathcal{M}(\theta_k)$  predicts the near-optimal solution for each task parameter  $\theta_k^2$ . The related optimization performance can be denoted as:

$$F_u(\theta_k) = f(\mathcal{M}(\theta_k), \theta_k), \forall u \in [U] \quad (18)$$

Then, the optimization results in  $\{F_u(\theta_k)\}_{k=1}^K$  are ranked, and the quantile values are computed as follows:

$$P_{\alpha,u} = \text{Quantile}_\alpha(F_u(\theta_k); \theta_k \in \bar{\Theta}) \quad (19)$$

where  $\alpha \in \{0.05, 0.25, 0.50, 0.75, 0.95\}$ . The final performance metric for each quantile is the mean value across all trials:

$$\bar{P}_\alpha = \frac{1}{U} \sum_{u=1}^U P_{\alpha,u}, \alpha \in \{0.05, 0.25, 0.50, 0.75, 0.95\}. \quad (20)$$

This metric provides a detailed understanding of the optimization performance of the task model across all the sampled task parameters. In this paper,  $K$  is set to  $100^2$  for task parameters in 2-dimensional space,  $K$  is set to  $10^5$  for task parameters

in 5-dimensional space and  $K$  is set to  $V^{20}$  for the other  $V$ -dimensional task parameter spaces.

### C. Results on Synthetic Problems

We assess the effectiveness of our methods using synthetic problems based on canonical objective functions modified with task parameters. Specifically, the objective function is defined as:

$$f(\mathbf{x}, \boldsymbol{\theta}) = g(\lambda(\mathbf{x} - \boldsymbol{\sigma}(L\boldsymbol{\theta}))) \quad (21)$$

where  $g(\cdot)$  is a base objective function, such as continuous optimization functions including Sphere, Ackley, Rastrigin, and Griewank to model the optimization problem,  $\mathbf{x}$  represents the decision variable within a  $V$ -dimensional space,  $\boldsymbol{\theta}$  denotes the task parameter within a  $D$ -dimensional space,  $\lambda > 0$  is a scaling factor to adjust the magnitude of decision variables,  $L \in \mathbb{R}^{V \times D}$  is a linear transformation matrix that maps task parameters into the  $V$ -dimensional space, and  $\boldsymbol{\sigma}$  represents a nonlinear transformation applied to the transformed task parameter. Totally, we construct eight synthetic problems: Sphere-I, Sphere-II, Ackley-I, Ackley-II, Rastrigin-I, Rastrigin-II, Griewank-I, and Griewank-II. Comprehensive details about these problems are provided in Section S-I of the supplementary materials.

TABLE I summarizes the optimization results across all sampled task parameters for each quantile, comparing GP-based optimization, PMTO, and  $(\theta_l, \theta_u)$ -PMTO. Notably,  $(\theta_l, \theta_u)$ -PMTO outperforms the other methods in 33 out of 40 quantiles, highlighting its generalizability in achieving better optimization results across the task parameter distribution. Moreover, PMTO-FT surpasses its single-task counterpart, GP-based optimization, in 32 out of 40 quantiles, demonstrating the benefits of incorporating task parameters for faster convergence and improved solutions empirically. According to Fig. 2, which depicts the convergence performance on

<sup>2</sup>For the final obtained task model of  $(\theta_l, \theta_u)$ -PMTO, only top  $p\%$  of the near-optimal solutions are employed to train the task model, where  $p$  is set to 70 in this paper.



TABLE I  
COMPARATIVE RESULTS ON SYNTHETIC PROBLEMS OVER 20 INDEPENDENT RUNS.

Problems	Quantile	GP-based Optimization	PMTO-FT	$(\theta_l, \theta_u)$ -PMTO-RT	$(\theta_l, \theta_u)$ -PMTO
Sphere-I	5%	3.4605e-02 (2.2632e-02) $\approx$	<b>3.3402e-02 (2.6492e-02) <math>\approx</math></b>	8.7646e-02 (6.5269e-02) $-$	4.3264e-02 (1.6935e-02)
	25%	1.2633e-01 (7.6585e-02) $\approx$	<b>1.2448e-01 (1.1445e-01) <math>\approx</math></b>	2.7083e-01 (2.2507e-01) $-$	1.2737e-01 (5.0277e-02)
	50%	2.9818e-01 (1.5592e-01) $\approx$	3.1267e-01 (2.8268e-01) $\approx$	5.8800e-01 (5.7331e-01) $-$	<b>2.4507e-01 (1.0836e-01)</b>
	75%	8.9086e-01 (3.0498e-01) $-$	6.5575e-01 (3.6466e-01) $-$	1.2854e+00 (1.2831e+00) $-$	<b>4.3753e-01 (2.3145e-01)</b>
	95%	3.4692e+00 (6.0544e-01) $-$	2.5749e+00 (1.0022e+00) $-$	3.3264e+00 (2.8819e+00) $-$	<b>8.3653e-01 (4.1045e-01)</b>
Sphere-II	5%	1.2980e+00 (8.1092e-02) $-$	1.3668e+00 (4.8590e-02) $-$	1.0247e+00 (2.8961e-01) $-$	<b>4.2056e-01 (2.5906e-01)</b>
	25%	2.2877e+00 (8.6464e-02) $-$	2.1996e+00 (2.2345e-02) $-$	1.9613e+00 (2.8010e-01) $-$	<b>1.1867e+00 (5.3394e-01)</b>
	50%	3.2896e+00 (1.7396e-01) $-$	3.0190e+00 (5.2262e-02) $-$	2.8556e+00 (2.7824e-01) $-$	<b>2.0908e+00 (7.1504e-01)</b>
	75%	4.5694e+00 (3.5324e-01) $-$	4.0215e+00 (1.0754e-01) $\approx$	3.9965e+00 (3.1599e-01) $\approx$	<b>3.3347e+00 (1.0237e+00)</b>
	95%	6.9576e+00 (1.0843e+00) $\approx$	5.6836e+00 (2.4876e-01) $\approx$	6.0923e+00 (5.4639e-01) $\approx$	<b>5.6729e+00 (2.1257e+00)</b>
Ackley-I	5%	2.1040e+00 (1.8214e-01) $-$	<b>9.6333e-02 (1.8901e-02) <math>\approx</math></b>	1.7585e-01 (1.2440e-01) $-$	9.7543e-02 (3.9146e-02)
	25%	2.9738e+00 (1.8514e-01) $-$	2.0568e-01 (3.5956e-02) $\approx$	5.2164e-01 (5.8015e-01) $-$	<b>2.0331e-01 (7.4606e-02)</b>
	50%	3.5819e+00 (1.6709e-01) $-$	3.5220e-01 (5.6119e-02) $\approx$	7.7263e-01 (7.7222e-01) $-$	<b>3.2185e-01 (1.1253e-01)</b>
	75%	4.5056e+00 (1.1115e-01) $-$	6.7452e-01 (1.0479e-01) $-$	9.9810e-01 (7.4903e-01) $-$	<b>4.8967e-01 (1.7913e-01)</b>
	95%	6.0673e+00 (2.1242e-01) $-$	2.0580e+00 (1.5660e-02) $-$	1.9350e+00 (1.6146e+00) $-$	<b>9.1072e-01 (4.9060e-01)</b>
Ackley-II	5%	3.6226e+00 (1.7790e-01) $-$	3.7061e+00 (4.6585e-02) $-$	3.4072e+00 (2.8914e-01) $-$	<b>2.5089e+00 (7.6250e-01)</b>
	25%	4.3273e+00 (1.9539e-01) $-$	4.2669e+00 (6.6596e-02) $-$	4.0061e+00 (1.9874e-01) $\approx$	<b>3.5385e+00 (7.6554e-01)</b>
	50%	4.9140e+00 (2.6313e-01) $\approx$	4.6222e+00 (6.0964e-02) $\approx$	4.4228e+00 (1.6292e-01) $\approx$	<b>4.3123e+00 (8.1509e-01)</b>
	75%	5.5161e+00 (2.7997e-01) $\approx$	5.2040e+00 (1.5259e-01) $\approx$	4.9905e+00 (2.3661e-01) $\approx$	<b>4.9644e+00 (8.1048e-01)</b>
	95%	6.4260e+00 (4.2145e-01) $\approx$	5.8336e+00 (1.3509e-01) $\approx$	<b>5.6838e+00 (2.5812e-01) <math>\approx</math></b>	5.8641e+00 (7.5154e-01)
Rastrigin-I	5%	2.6359e+01 (6.2784e+00) $\approx$	<b>2.5169e+01 (2.6266e+00) <math>\approx</math></b>	2.7618e+01 (3.6902e+00) $\approx$	2.6238e+01 (2.5165e+00)
	25%	4.4250e+01 (7.7101e+00) $\approx$	<b>4.2094e+01 (3.1510e+00) <math>\approx</math></b>	4.4928e+01 (5.5935e+00) $\approx$	4.2326e+01 (3.6744e+00)
	50%	5.9753e+01 (1.0151e+01) $-$	5.6112e+01 (3.9190e+00) $\approx$	5.9310e+01 (8.8632e+00) $\approx$	<b>5.4785e+01 (5.4205e+00)</b>
	75%	8.3515e+01 (1.8001e+01) $-$	7.4887e+01 (6.2412e+00) $-$	7.9073e+01 (1.9286e+01) $-$	<b>6.8098e+01 (8.2728e+00)</b>
	95%	1.5818e+02 (4.3552e+01) $-$	1.3682e+02 (2.2979e+01) $-$	1.2808e+02 (5.8301e+01) $-$	<b>8.9259e+01 (1.5389e+01)</b>
Rastrigin-II	5%	6.4737e+01 (1.7582e+00) $-$	6.3057e+01 (2.2005e+00) $-$	6.1093e+01 (2.8075e+00) $-$	<b>4.5054e+01 (6.0348e+00)</b>
	25%	9.7163e+01 (3.5574e+00) $-$	9.3105e+01 (2.6550e+00) $-$	9.6881e+01 (4.1387e+00) $-$	<b>7.1361e+01 (1.1557e+01)</b>
	50%	1.2564e+02 (6.9602e+00) $-$	1.1905e+02 (3.9188e+00) $-$	1.2988e+02 (9.3123e+00) $-$	<b>9.4798e+01 (1.6858e+01)</b>
	75%	1.6150e+02 (1.3363e+01) $-$	1.5109e+02 (6.5386e+00) $-$	1.6934e+02 (1.5657e+01) $-$	<b>1.2334e+02 (2.3236e+01)</b>
	95%	2.2799e+02 (2.9678e+01) $-$	2.0929e+02 (1.4155e+01) $\approx$	2.3501e+02 (2.6453e+01) $-$	<b>1.7181e+02 (3.4438e+01)</b>
Griewank-I	5%	1.4295e+00 (3.6791e-01) $\approx$	<b>1.2337e+00 (1.7745e-01) <math>\approx</math></b>	1.5408e+00 (2.4038e-01) $-$	1.3317e+00 (1.5637e-01)
	25%	2.9319e+00 (1.5217e+00) $-$	2.1563e+00 (6.2049e-01) $\approx$	2.6166e+00 (5.5361e-01) $-$	<b>2.0979e+00 (4.5880e-01)</b>
	50%	5.6758e+00 (3.7501e+00) $-$	3.7437e+00 (1.3372e+00) $\approx$	4.1832e+00 (1.1701e+00) $-$	<b>3.0935e+00 (1.0398e+00)</b>
	75%	1.1592e+01 (7.4868e+00) $-$	7.8351e+00 (2.3734e+00) $-$	7.8516e+00 (3.4542e+00) $-$	<b>4.7885e+00 (1.9504e+00)</b>
	95%	2.8449e+01 (1.2148e+01) $-$	2.4819e+01 (5.0000e+00) $-$	1.9363e+01 (1.1093e+01) $-$	<b>8.5325e+00 (4.3527e+00)</b>
Griewank-II	5%	8.5584e+00 (4.8922e-01) $-$	8.1302e+00 (5.1623e-01) $-$	6.7492e+00 (1.2233e+00) $-$	<b>4.0665e+00 (1.3843e+00)</b>
	25%	1.3381e+01 (6.6195e-01) $-$	1.3655e+01 (1.6315e-01) $-$	1.2651e+01 (1.6883e+00) $-$	<b>9.0974e+00 (3.1722e+00)</b>
	50%	1.8848e+01 (1.3946e+00) $-$	1.9214e+01 (5.9426e-01) $-$	1.8282e+01 (2.5765e+00) $\approx$	<b>1.4656e+01 (4.2747e+00)</b>
	75%	2.5659e+01 (2.6930e+00) $\approx$	2.6220e+01 (8.5712e-01) $\approx$	2.5084e+01 (3.7183e+00) $\approx$	<b>2.2094e+01 (5.0576e+00)</b>
	95%	3.7448e+01 (6.2271e+00) $\approx$	3.8192e+01 (1.5611e+00) $\approx$	3.7894e+01 (6.7145e+00) $\approx$	<b>3.5562e+01 (6.5583e+00)</b>

sample tasks in two exemplified synthetic problems, PMTO-FT achieves better empirical convergence results compared to the single-task counterpart. This improvement contributes to the superior task model performance observed in TABLE I and verifies the theory analysis provided in Section IV-B. Additionally, TABLE I includes results for a  $(\theta_l, \theta_u)$ -PMTO-RT variant, which replaces the strategic task evolution module with randomly generating a task parameter per iteration. Serving as an ablation study, the proposed method significantly outperforms this random search variant in most quantiles, underscoring the effectiveness of the task evolution module in actively exploring the task space during optimization. These findings highlight the effectiveness of  $(\theta_l, \theta_u)$ -PMTO.

#### D. Case Study in Adaptive Control System

1) *Robot Arm Optimization Problem:* As shown in Fig. 3(a), the robot arm optimization problem is to adjust the angular positions of the joints to bring the end effector as close as possible to the target position<sup>3</sup>. Here, the distance

between the end effector and the target position is considered the objective function, while the angular positions of the joints serve as the solution (i.e.,  $\alpha_1, \alpha_2, \alpha_3$  in Fig. 3(a)). The task space includes task parameter  $L$  bounded by  $[0.5/n, 1/n]$  and  $\alpha_{max}$  bounded by  $[0.5\pi/n, \pi/n]$ , where  $L$  is the length of each arm,  $\alpha_{max}$  identifies the maximal range of the rotation of each joint, and  $n$  is the number of joints set to  $n = 3$  in our case study. The position of the first joint attached to the ground is set as  $[0, 0]$  while the target position is fixed to  $[0.5, 0.5]$  for all optimization tasks. As shown in TABLE II and Fig. 4(a), compared to GP-based optimization, PMTO-FT can stably achieve better optimization performance for the 50%, 75%, 95% quantile optimization results, whereas for the best cases 5% and 25%, both optimization methods in the fixed set of tasks do not show significant difference. The fixed-task methods are limited by constrained task environments, hindering optimization results. In contrast, by enabling the joint search in the solution space and the task space, the proposed  $(\theta_l, \theta_u)$ -PMTO leverages related tasks to enhance convergence and achieve better objective values in best case

<sup>3</sup>One can refer to [11] for the exact formulation of the objective function.

TABLE II  
COMPARATIVE RESULTS ON ADAPTIVE CONTROL SYSTEMS OVER 20 INDEPENDENT RUNS

Problems	Quantile	GP-based Optimization	PMTO-FT	$(\theta_l, \theta_u)$ -PMTO
Robot Arm	5%	4.2821e-02 (1.9260e-02) –	3.4766e-02 (7.9264e-03) –	<b>1.7336e-02 (5.2244e-03)</b>
	25%	8.9019e-02 (2.5297e-02) –	7.6430e-02 (1.7672e-02) –	<b>4.7606e-02 (1.4060e-02)</b>
	50%	1.3401e-01 (2.0803e-02) –	1.0522e-01 (2.0310e-02) –	<b>7.5639e-02 (1.6956e-02)</b>
	75%	1.7645e-01 (1.5028e-02) –	1.3607e-01 (1.9514e-02) $\approx$	<b>1.1816e-01 (1.8595e-02)</b>
	95%	2.3556e-01 (1.6606e-02) –	1.7845e-01 (1.4280e-02) $\approx$	<b>1.7742e-01 (8.5307e-03)</b>
Crane Load-I	5%	3.0679e+04 (5.7316e+04) –	1.4233e+03 (1.3452e+03) –	<b>4.6175e+02 (3.2924e+02)</b>
	25%	1.1283e+05 (1.4729e+05) –	2.7508e+04 (2.0614e+04) –	<b>1.0081e+04 (4.3555e+03)</b>
	50%	2.1993e+05 (2.1653e+05) –	1.0485e+05 (7.1414e+04) –	<b>3.9601e+04 (1.2591e+04)</b>
	75%	3.7102e+05 (2.9138e+05) –	2.6922e+05 (1.6376e+05) –	<b>1.4146e+05 (1.2170e+05)</b>
	95%	6.0364e+05 (3.7526e+05) $\approx$	6.1116e+05 (3.8202e+05) $\approx$	<b>3.4578e+05 (3.2520e+05)</b>
Crane Load-II	5%	6.3392e+02 (3.5072e+02) –	4.7310e+02 (1.1462e+02) –	<b>1.5026e+02 (7.6382e+01)</b>
	25%	1.6577e+04 (9.7445e+03) –	1.1846e+04 (3.3891e+03) –	<b>3.0218e+03 (9.1541e+02)</b>
	50%	7.4319e+04 (4.7370e+04) –	5.7356e+04 (1.8227e+04) –	<b>1.1835e+04 (2.1282e+03)</b>
	75%	1.7974e+05 (9.7858e+04) –	1.6482e+05 (5.2057e+04) –	<b>2.9978e+04 (7.5976e+03)</b>
	95%	3.9408e+05 (2.0022e+05) –	3.8901e+05 (1.1719e+05) –	<b>8.8104e+04 (3.5100e+04)</b>

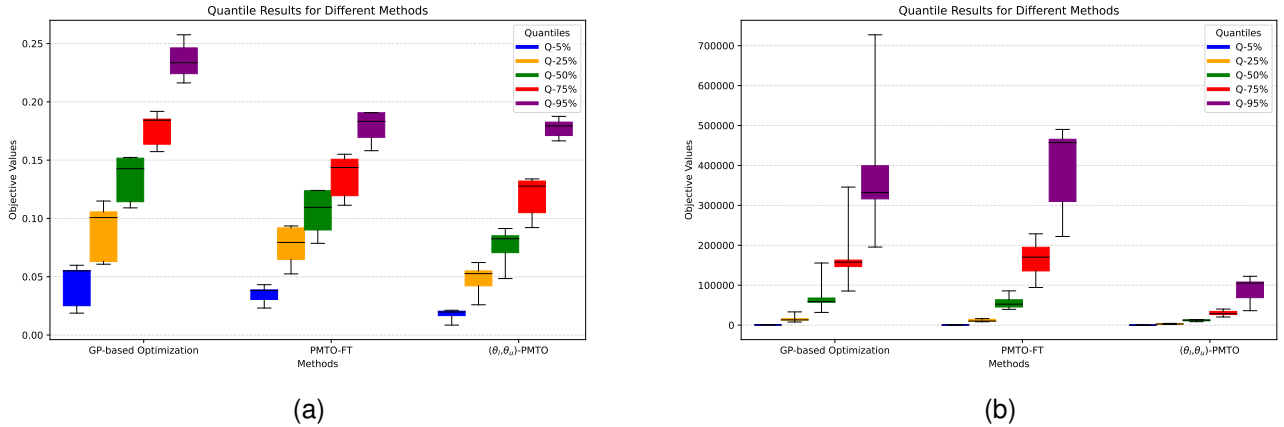


Fig. 4. The comparative results on adaptive control problems: (a) Robot arm optimization under distinct operating conditions (b) Crane-load system optimization under distinct environments.

5% optimization results and enhance the moderately worse case optimization results (25% and 50%) as well.

2) *Crane-Load System Optimization with Time Delays (Crane Load-I)*: As shown in Fig. 3(b), we consider optimizing a crane-load system control problem [60]. The goal is to accelerate the system with crane  $m_1$  and load  $m_2$  by an external drive force  $F$  to achieve a target velocity with minimal time and oscillation. The solutions for this control system are shown in Fig. 3(b), where  $t_1, t_2, t_3$  are decision variables to switch the drive force  $F$  during the control process. In actual operating conditions, however, time delays in the control system can arise from environmental uncertainties and they can destabilize the entire system and induce oscillations [61]. Therefore, the task space includes the possible time delays  $\Delta t_1, \Delta t_2, \Delta t_3$  for each time interval. As shown in TABLE II, under various time delays, PMTO-FT can achieve a more stable system control compared to the GP-based optimization, exhibiting the power of multi-task optimization enabled by the inclusion of task parameters in the optimization loop. Moreover, with the additional capability of the joint search in both solution and task spaces, optimization results in different quantiles can be significantly enhanced by

the proposed  $(\theta_l, \theta_u)$ -PMTO.

3) *Crane-Load System Optimization with Diverse Operating Conditions (Crane Load-II)*: Here, we still consider optimizing the control problem for the crane-load system in Fig. 3(b) to accelerate the system with crane  $m_1$  and load  $m_2$  by an external drive force  $F$  to achieve a target velocity with minimal time and oscillation. Differently, we introduce a distinct task space including the diverse operating conditions. Diverse types of suspension  $l$ , loads  $m_2$ , and resistance  $W$  for a fixed crane can occur due to distinct operating conditions and environments. Therefore, we consider identifying the optimal solutions for diverse possible tuples of  $(l, m_2, W)$  in a bounded continuous task space. Although in a different context, optimization results under distinct environment factors can still be enhanced by PMTO-FT, attributing the merits to the synergies across the system optimization under various operating conditions. Empowered by *task evolution*, as depicted in TABLE II and Fig. 4(b), the joint search across solution and task spaces can further enhance the optimization results across all the quantiles, showing  $(\theta_l, \theta_u)$ -PMTO's ability to stabilize the crane-load system under diverse operating conditions.

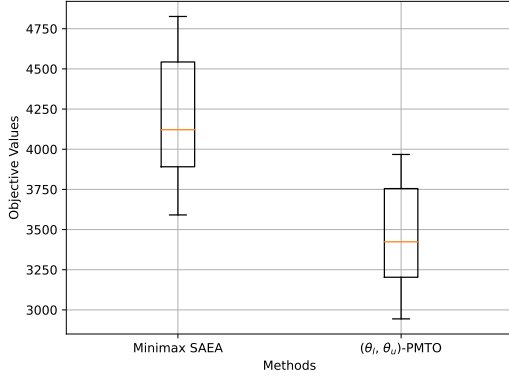


Fig. 5. The comparative result for the minimax optimization problem. The optimal solution is generated by the baseline minimax solver and  $(\theta_l, \theta_u)$ -PMTO algorithm. The objective values of the generated design under various processing errors are exhibited.

### E. Case Study in Robust Engineering Design

In this case study, we address a robust engineering design problem as shown in Fig. 3(c), where the objective is to minimize the aggregated function of both the structural weight and joint displacement of the truss by optimizing the lengths of two bars  $\theta_1$  and  $\theta_2$ . However, due to the existing processing errors, even when the length of bars are designed as  $\theta = (\theta_1, \theta_2)$ , the operating truss structure obtained after actual processing may deviate from the original design. Let this processing error be represented by  $\mathbf{x} = (x_1, x_2)$  so that the operating structural parameters are  $(\theta + \mathbf{x})$ . In robust optimization, the design problem we aim to solve can then be formulated as:

$$\min_{\theta} \max_{\mathbf{x}} f(\mathbf{x}, \theta). \quad (22)$$

Consequently, we show that PMTO can be an effective approach to solve this minimax optimization problem. We reformulate the minimax problem (22) by treating the original design variables  $\theta$  as task parameters and the processing error  $\mathbf{x}$  as the decision vector. As per the formulation (3), a task model can be constructed in PMTO to estimate the worst-case processing error corresponding to each design variable by  $\mathbf{x}^* = \mathcal{M}(\theta)$ . This obtained task model supports to solve the problem (22) as  $\min_{\theta} f(\mathcal{M}(\theta), \theta)$ . Thereafter, the minimax optimization shown as (22) can be solved by the PMTO.

As shown in Fig. 5, we compare  $(\theta_l, \theta_u)$ -PMTO to a popular minimax optimization solver, Minimax SAEA [13]. To evaluate the robustness of the generated design, we impose many possible processing errors (800 randomly processing errors) on the generated design from both Minimax SAEA and  $(\theta_l, \theta_u)$ -PMTO. As shown in Fig. 5,  $(\theta_l, \theta_u)$ -PMTO can generate a relatively more robust plain truss design, showing that the proposed  $(\theta_l, \theta_u)$ -PMTO can serve as a generic tool to solve minimax optimization as well.

## VII. CONCLUSION

This paper introduces PMTO as a novel generalization of MTO from a fixed and finite set of tasks to infinite task sets. The proposed  $(\theta_l, \theta_u)$ -PMTO algorithm enables joint

exploration of continuous solution and task spaces through two key approximations: mapping the solution space to the objective space for inter-task transfer and mapping the task space to the solution space to target under-explored regions. Experimental results demonstrate two main benefits. First, incorporating continuous task parameters as a medium for knowledge transfer accelerates multi-task optimization and improves convergence. Second, an evolutionary exploration empowered by a calibrated task model in the joint solution-task space enhances the use of information from under-explored areas, boosting overall optimization efficiency.

Despite these advancements, our study primarily addresses low- to moderate-dimensional problems, reflecting the inherent limitations of GP models in high-dimensional search spaces. Enhancing the scalability of PMTO methods to extend their applicability to higher-dimensional optimization problems remains a crucial direction for future work. Additionally, the application of PMTO to multi-objective optimization settings remains an open problem and represents another promising avenue for future exploration.

## APPENDIX

### PROOF OF THE THEOREM

*Proof:* Given the dataset  $\mathcal{D}_{pmt}$ , in the multivariate Gaussian case, the *conditional information gain* about the objective function corresponding to arbitrary parameterized task of interest  $m^* \in [M]$  is:

$$I([y^{(1)}, \dots, y^{(T)}]; \mathbf{f}_{m^*} | \mathcal{D}_{pmt}) = \frac{1}{2} \log |\mathbf{I} + \sigma_{\epsilon}^{-2} \mathbf{K}_{pmt, m^*}|, \quad (23)$$

where  $\mathbf{K}_{pmt, m^*}$  denotes the conditional covariance matrix for the parameterized task  $m^*$ , derived from the dataset  $\mathcal{D}_{pmt}$ , which includes data from all tasks. Next, we show how to calculate  $\mathbf{K}_{pmt, m^*}$ . Let  $\pi_i, i \in [M]$  represents a rearrangement of the values  $\{1, 2, \dots, M\}$ , then  $\mathbf{K}_{pmt}$  can be further denoted as follows:

$$\mathbf{K}_{pmt} = \begin{bmatrix} \mathbf{K}_{\pi_1, \pi_1} & \mathbf{K}_{\pi_1, \pi_2} & \cdots & \mathbf{K}_{\pi_1, \pi_M} \\ \mathbf{K}_{\pi_2, \pi_1} & \mathbf{K}_{\pi_2, \pi_2} & \cdots & \mathbf{K}_{\pi_2, \pi_M} \\ \vdots & \vdots & \ddots & \vdots \\ \mathbf{K}_{\pi_M, \pi_1} & \mathbf{K}_{\pi_M, \pi_2} & \cdots & \mathbf{K}_{\pi_M, \pi_M} \end{bmatrix}, \quad (24)$$

where each block matrix  $\mathbf{K}_{i,j} \in \mathbb{R}^{T \times T}$  can be defined as follows:

$$\mathbf{K}_{i,j} = \begin{bmatrix} \kappa((\mathbf{x}_{1,i}, \theta_i), (\mathbf{x}_{1,j}, \theta_j)) & \cdots & \kappa((\mathbf{x}_{1,i}, \theta_i), (\mathbf{x}_{T,j}, \theta_j)) \\ \vdots & \ddots & \vdots \\ \kappa((\mathbf{x}_{T,i}, \theta_i), (\mathbf{x}_{1,j}, \theta_j)) & \cdots & \kappa((\mathbf{x}_{T,i}, \theta_i), (\mathbf{x}_{T,j}, \theta_j)) \end{bmatrix}. \quad (25)$$

Without loss of generality, let  $\pi_M = m^*$ ,

$$\mathbf{K}_{\setminus m^*} = \begin{bmatrix} \mathbf{K}_{\pi_1, \pi_1} & \cdots & \mathbf{K}_{\pi_1, \pi_{M-1}} \\ \vdots & \ddots & \vdots \\ \mathbf{K}_{\pi_{M-1}, \pi_1} & \cdots & \mathbf{K}_{\pi_{M-1}, \pi_{M-1}} \end{bmatrix}, \quad (26)$$

and  $B = [\mathbf{K}_{\pi_M, \pi_1} \quad \mathbf{K}_{\pi_M, \pi_2} \quad \cdots \quad \mathbf{K}_{\pi_M, \pi_M}]^T$ , then we can further formulate  $\mathbf{K}_{pmt}$  as:

$$\mathbf{K}_{pmt} = \begin{bmatrix} \mathbf{K}_{\setminus m^*} & B \\ B^T & \mathbf{K}_{m^*, m^*} \end{bmatrix}. \quad (27)$$

Using the properties of the conditional Gaussian distribution,  $\mathbf{K}_{pmt,m^*}$  can be calculated as:

$$\mathbf{K}_{pmt,m^*} = \mathbf{K}_{m^*,m^*} - B^T(\mathbf{K}_{\setminus m^*} + \sigma_\epsilon^{-2}\mathbf{I})^{-1}B. \quad (28)$$

Likewise, in terms of the independent strategy, the corresponding conditional information gain is

$$I([y^{(1)}, \dots, y^{(T)}]; \mathbf{f}_{m^*} | \mathcal{D}_{m^*}) = \frac{1}{2} \log |\mathbf{I} + \sigma_\epsilon^{-2}\mathbf{K}_{ind,m^*}|, \quad (29)$$

where  $\mathbf{K}_{ind,m^*}$  is the covariance matrix with all the samples in  $\mathcal{D}_{m^*}$ . Based on the assumption on the kernel function that  $\kappa_{pmt}((\mathbf{x}, \boldsymbol{\theta}_m), (\mathbf{x}', \boldsymbol{\theta}_m)) = \kappa_{ind}(\mathbf{x}, \mathbf{x}')$ , it follows that  $\mathbf{K}_{ind,m^*} = \mathbf{K}_{m^*,m^*}$ . This can further help us to analyze the relationship of the two conditional information gains. Since the covariance matrix  $\mathbf{K}_{pmt}$ ,  $\mathbf{K}_{\setminus m^*}$  and  $\mathbf{K}_{m^*,m^*}$  are both positive semi-definite (PSD), then according to the *Schur complement theorem* [62], we know  $\mathbf{K}_{m^*,m^*} - B^T(\mathbf{K}_{\setminus m^*} + \sigma_\epsilon^{-2}\mathbf{I})^{-1}B$  and  $\mathbf{K}_{\setminus m^*} + \sigma_\epsilon^{-2}\mathbf{I}$  are also PSD. Then, considering the *Minkowski determinant inequality* that for PSD matrices  $C$  and  $D$ , we have  $|C+D| \geq |C|+|D| \geq |C|$ . Substituting  $C$  and  $D$  by  $C = \mathbf{I} + \sigma_\epsilon^{-2}\mathbf{K}_{pmt,m^*}$  and  $D = \mathbf{I} + \sigma_\epsilon^{-2}B^T(\mathbf{K}_{\setminus m^*} + \sigma_\epsilon^{-2}\mathbf{I})^{-1}B$ , respectively, then the follows can be obtained:

$$\begin{aligned} |\mathbf{I} + \sigma_\epsilon^{-2}\mathbf{K}_{m^*,m^*}| &= |\mathbf{I} + \sigma_\epsilon^{-2}\mathbf{K}_{ind,m^*}| \\ &\geq |\mathbf{I} + \sigma_\epsilon^{-2}\mathbf{K}_{pmt,m^*}|. \end{aligned} \quad (30)$$

This results in the fact that

$$\begin{aligned} I([y^{(1)}, \dots, y^{(T)}]; \mathbf{f}_{m^*} | \mathcal{D}_{m^*}) \\ \geq I([y^{(1)}, \dots, y^{(T)}]; \mathbf{f}_{m^*} | \mathcal{D}_{pmt}). \end{aligned} \quad (31)$$

Hence, we can deduce from (31) that  $\gamma_{T,m^*} \leq \hat{\gamma}_{T,m^*}^{ind}$ . ■

## REFERENCES

- [1] A. Gupta, Y. Ong, and L. Feng, "Insights on transfer optimization: Because experience is the best teacher," *IEEE Trans. on Emerg. Topics in Comput. Intell.*, vol. 2, no. 1, pp. 51–64, 2018.
- [2] A. Gupta, Y.-S. Ong, and L. Feng, "Multifactorial evolution: toward evolutionary multitasking," *IEEE Trans. on Evol. Comput.*, vol. 20, no. 3, pp. 343–357, 2016.
- [3] K. Swersky, J. Snoek, and R. P. Adams, "Multi-task bayesian optimization," in *Advances in Neural Information Processing Systems*, C. Burges, L. Bottou, M. Welling, Z. Ghahramani, and K. Weinberger, Eds., vol. 26. Curran Associates, Inc., 2013.
- [4] K. K. Bali, Y.-S. Ong, A. Gupta, and P. S. Tan, "Multifactorial evolutionary algorithm with online transfer parameter estimation: Mfea-ii," *IEEE Trans. on Evol. Comput.*, vol. 24, no. 1, pp. 69–83, 2019.
- [5] K. K. Bali, A. Gupta, L. Feng, Y. S. Ong, and T. P. Siew, "Linearized domain adaptation in evolutionary multitasking," in *2017 IEEE Congr. on Evol. Comput. (CEC)*, 2017, pp. 1295–1302.
- [6] L. Feng, L. Zhou, J. Zhong, A. Gupta, Y.-S. Ong, K.-C. Tan, and A. K. Qin, "Evolutionary multitasking via explicit autoencoding," *IEEE Trans. on Cybern.*, vol. 49, no. 9, pp. 3457–3470, 2018.
- [7] A. D. Martinez, J. Del Ser, E. Osaba, and F. Herrera, "Adaptive multifactorial evolutionary optimization for multitask reinforcement learning," *IEEE Trans. on Evol. Comput.*, vol. 26, no. 2, pp. 233–247, 2022.
- [8] J. Zhong, L. Feng, W. Cai, and Y. S. Ong, "Multifactorial genetic programming for symbolic regression problems," *IEEE Trans. on Syst., Man, and Cybern.: Syst.*, vol. 50, no. 11, pp. 4492–4505, 2020.
- [9] T. Rios, B. van Stein, T. Bäck, B. Sendhoff, and S. Menzel, "Multitask shape optimization using a 3d point cloud autoencoder as unified representation," *IEEE Trans. on Evol. Comput.*, pp. 1–1, 2021.
- [10] A. Gupta, L. Zhou, Y.-S. Ong, Z. Chen, and Y. Hou, "Half a dozen real-world applications of evolutionary multitasking, and more," *IEEE Comput. Intell. Mag.*, vol. 17, no. 2, pp. 49–66, 2022.
- [11] J.-B. Mouret and G. Maguire, "Quality diversity for multi-task optimization," in *Proceedings of the 2020 Genetic and Evol. Comput. Conference*, ser. GECCO '20. New York, NY, USA: Association for Computing Machinery, 2020, p. 121–129.
- [12] A. Cully, J. Clune, D. Tarapore, and J.-B. Mouret, "Robots that can adapt like animals," *Nature*, vol. 521, no. 7553, pp. 503–507, May 2015. [Online]. Available: <https://doi.org/10.1038/nature14422>
- [13] A. Zhou and Q. Zhang, "A surrogate-assisted evolutionary algorithm for minimax optimization," in *IEEE Congr. on Evol. Comput.*, 2010, pp. 1–7.
- [14] A. Gupta, J. Mańdziuk, and Y.-S. Ong, "Evolutionary multitasking in bi-level optimization," *Complex & Intelligent Syst.*, vol. 1, no. 1-4, pp. 83–95, 2015.
- [15] E. V. Bonilla, K. Chai, and C. Williams, "Multi-task gaussian process prediction," in *Advances in Neural Information Processing Systems*, J. Platt, D. Koller, Y. Singer, and S. Roweis, Eds., vol. 20. Curran Associates, Inc., 2007.
- [16] P. G. Sessa, P. Laforge, N. Cesa-Bianchi, and A. Krause, "Multitask learning with no regret: from improved confidence bounds to active learning," in *Advances in Neural Information Processing Systems*, A. Oh, T. Naumann, A. Globerson, K. Saenko, M. Hardt, and S. Levine, Eds., vol. 36. Curran Associates, Inc., 2023, pp. 6770–6781.
- [17] J. Lübsen, C. Hesse, and A. Eichler, "Towards safe multi-task Bayesian optimization," in *Proceedings of the 6th Annual Learning for Dynamics Control Conference*, ser. Proceedings of Machine Learning Research, vol. 242. PMLR, 15–17 Jul 2024, pp. 839–851.
- [18] T. Wei, S. Wang, J. Zhong, D. Liu, and J. Zhang, "A review on evolutionary multitask optimization: Trends and challenges," *IEEE Trans. on Evol. Comput.*, vol. 26, no. 5, pp. 941–960, 2022.
- [19] Y. Yuan, Y.-S. Ong, L. Feng, A. K. Qin, A. Gupta, B. Da, Q. Zhang, K. C. Tan, Y. Jin, and H. Ishibuchi, "Evolutionary multitasking for multiobjective continuous optimization: Benchmark problems, performance metrics and baseline results," *arXiv preprint arXiv:1706.02766*, 2017.
- [20] K. K. Bali, A. Gupta, Y.-S. Ong, and P. S. Tan, "Cognizant multitasking in multiobjective multifactorial evolution: Mo-mfea-ii," *IEEE Trans. on Cybern.*, vol. 51, no. 4, pp. 1784–1796, 2021.
- [21] B. Da, A. Gupta, Y.-S. Ong, and L. Feng, "Evolutionary multitasking across single and multi-objective formulations for improved problem solving," in *2016 IEEE Congr. on Evol. Comput. (CEC)*, 2016, pp. 1695–1701.
- [22] Y. Huang, W. Zhou, Y. Wang, M. Li, L. Feng, and K. C. Tan, "Evolutionary multitasking with centralized learning for large-scale combinatorial multiobjective optimization," *IEEE Trans. on Evol. Comput.*, vol. 28, no. 5, pp. 1499–1513, 2024.
- [23] L. Feng, Y. Huang, L. Zhou, J. Zhong, A. Gupta, K. Tang, and K. C. Tan, "Explicit evolutionary multitasking for combinatorial optimization: A case study on capacitated vehicle routing problem," *IEEE Trans. on Cybern.*, vol. 51, no. 6, pp. 3143–3156, 2021.
- [24] A. Gupta, Y.-S. Ong, L. Feng, and K. C. Tan, "Multiobjective multifactorial optimization in evolutionary multitasking," *IEEE Trans. on Cybern.*, vol. 47, no. 7, pp. 1652–1665, 2016.
- [25] J. Ding, C. Yang, Y. Jin, and T. Chai, "Generalized multitasking for evolutionary optimization of expensive problems," *IEEE Trans. on Evol. Comput.*, vol. 23, no. 1, pp. 44–58, 2017.
- [26] D. Wu and X. Tan, "Multitasking genetic algorithm (mtga) for fuzzy system optimization," *IEEE Trans. on Fuzzy Syst.*, vol. 28, no. 6, pp. 1050–1061, 2020.
- [27] Z. Liang, W. Liang, Z. Wang, X. Ma, L. Liu, and Z. Zhu, "Multiobjective evolutionary multitasking with two-stage adaptive knowledge transfer based on population distribution," *IEEE Trans. on Syst., Man, and Cybern.: Syst.*, vol. 52, no. 7, pp. 4457–4469, 2022.
- [28] Z. Tang, M. Gong, Y. Wu, W. Liu, and Y. Xie, "Regularized evolutionary multitask optimization: Learning to intertask transfer in aligned subspace," *IEEE Trans. on Evol. Comput.*, vol. 25, no. 2, pp. 262–276, 2021.
- [29] Z. Chen, Y. Zhou, X. He, and J. Zhang, "Learning task relationships in evolutionary multitasking for multiobjective continuous optimization," *IEEE Trans. on Cybern.*, pp. 1–12, 2020.
- [30] Z. Tang, M. Gong, Y. Wu, A. K. Qin, and K. C. Tan, "A multifactorial optimization framework based on adaptive intertask coordinate system," *IEEE Trans. on Cybern.*, vol. 52, no. 7, pp. 6745–6758, 2022.
- [31] R. Lim, A. Gupta, Y.-S. Ong, L. Feng, and A. N. Zhang, "Non-linear domain adaptation in transfer evolutionary optimization," *Cognitive Comput.*, vol. 13, pp. 290–307, 2021.
- [32] X. Wang, Q. Kang, M. Zhou, S. Yao, and A. Abusorrah, "Domain adaptation multitask optimization," *IEEE Trans. on Cybern.*, vol. 53, no. 7, pp. 4567–4578, 2023.

- [33] Z. Huang, Y. Mei, F. Zhang, and M. Zhang, "Multitask linear genetic programming with shared individuals and its application to dynamic job shop scheduling," *IEEE Trans. on Evol. Comput.*, pp. 1–1, 2023.
- [34] H. Li, Y.-S. Ong, M. Gong, and Z. Wang, "Evolutionary multitasking sparse reconstruction: Framework and case study," *IEEE Trans. on Evol. Comput.*, vol. 23, no. 5, pp. 733–747, 2019.
- [35] Y. Wu, H. Ding, M. Gong, A. K. Qin, W. Ma, Q. Miao, and K. C. Tan, "Evolutionary multiform optimization with two-stage bidirectional knowledge transfer strategy for point cloud registration," *IEEE Trans. on Evol. Comput.*, vol. 28, no. 1, pp. 62–76, 2024.
- [36] L. Feng, Q. Shang, Y. Hou, K. C. Tan, and Y.-S. Ong, "Multispace evolutionary search for large-scale optimization with applications to recommender systems," *IEEE Trans. on Artificial Intell.*, vol. 4, no. 1, pp. 107–120, 2023.
- [37] T. Anne and J.-B. Mouret, "Parametric-task map-elites," in *Proceedings of the Genetic and Evol. Comput. Conference*, ser. GECCO '24. New York, NY, USA: Association for Computing Machinery, 2024, p. 68–77.
- [38] I. Pappas, D. Kenefake, B. Burnak, S. Avraamidou, H. S. Ganesh, J. Katz, N. A. Diangelakis, and E. N. Pistikopoulos, "Multiparametric programming in process systems engineering: Recent developments and path forward," *Frontiers in Chemical Engineering*, vol. 2, 2021.
- [39] S. Barnett, "A simple class of parametric linear programming problems," *Operations Research*, vol. 16, no. 6, pp. 1160–1165, 1968.
- [40] V. M. Charitopoulos, L. G. Papageorgiou, and V. Dua, "Multi-parametric mixed integer linear programming under global uncertainty," *Computers & Chemical Engineering*, vol. 116, pp. 279–295, 2018.
- [41] E. N. Pistikopoulos, V. Dua, N. A. Bozinis, A. Bemporad, and M. Morari, "On-line optimization via off-line parametric optimization tools," *Computers & Chemical Engineering*, vol. 26, no. 2, pp. 175–185, 2002.
- [42] P. Dua, K. Kouramas, V. Dua, and E. Pistikopoulos, "Mpc on a chip—recent advances on the application of multi-parametric model-based control," *Computers & Chemical Engineering*, vol. 32, no. 4, pp. 754–765, 2008.
- [43] R. S. Vadamalu and C. Beidl, "Explicit mpc phev energy management using markov chain based predictor: Development and validation at engine-in-the-loop testbed," in *2016 European Control Conference (ECC)*, 2016, pp. 453–458.
- [44] J. Lee and H.-J. Chang, "Multi-parametric model predictive control for autonomous steering using an electric power steering system," *Proceedings of the Institution of Mechanical Engineers, Part D: Journal of Automobile Engineering*, vol. 233, no. 13, pp. 3391–3402, 2019.
- [45] C. Jia, X. Wang, K. Zhou, and D. Xianqing, "Sensorless explicit model predictive control for ipmsm drives," in *2019 IEEE 2nd International Conference on Automation, Electronics and Electrical Engineering (AUTEEE)*, 2019, pp. 82–87.
- [46] B. Scaglioni, L. Previtiera, J. Martin, J. Norton, K. L. Obstein, and P. Valdastrì, "Explicit model predictive control of a magnetic flexible endoscope," *IEEE Robotics and Automation Letters*, vol. 4, no. 2, pp. 716–723, 2019.
- [47] M. Seeger, "Gaussian processes for machine learning," *International journal of neural systems*, vol. 14, no. 02, pp. 69–106, 2004.
- [48] N. Srinivas, A. Krause, S. M. Kakade, and M. W. Seeger, "Information-theoretic regret bounds for gaussian process optimization in the bandit setting," *IEEE Trans. on Information Theory*, vol. 58, no. 5, pp. 3250–3265, 2012.
- [49] B. Shahriari, K. Swersky, Z. Wang, R. P. Adams, and N. de Freitas, "Taking the human out of the loop: A review of bayesian optimization," *Proceedings of the IEEE*, vol. 104, no. 1, pp. 148–175, 2016.
- [50] A. T. W. Min, A. Gupta, and Y.-S. Ong, "Generalizing transfer bayesian optimization to source-target heterogeneity," *IEEE Trans. Autom. Sci. Eng.*, vol. 18, no. 4, pp. 1754–1765, 2021.
- [51] D. Zhan and H. Xing, "Expected improvement for expensive optimization: a review," *Journal of Global Optimization*, vol. 78, no. 3, pp. 507–544, Nov 2020.
- [52] M. Pearce and J. Branke, "Continuous multi-task bayesian optimisation with correlation," *European Journal of Operational Research*, vol. 270, no. 3, pp. 1074–1085, 2018.
- [53] Z. Wang and S. Jegelka, "Max-value entropy search for efficient Bayesian optimization," in *Proceedings of the 34th International Conference on Machine Learning*, ser. Proceedings of Machine Learning Research, vol. 70. PMLR, 06–11 Aug 2017, pp. 3627–3635.
- [54] A. Kulesza and B. Taskar, "Determinantal point processes for machine learning," *Foundations and Trends® in Machine Learning*, vol. 5, no. 2–3, pp. 123–286, 2012.
- [55] J. Parker-Holder, A. Pacchiano, K. M. Choromanski, and S. J. Roberts, "Effective diversity in population based reinforcement learning," in *Advances in Neural Information Processing Systems*, vol. 33. Curran Associates, Inc., 2020, pp. 18 050–18 062.
- [56] K. Deb and D. Deb, "Analysing mutation schemes for real-parameter genetic algorithms," *International Journal of Artificial Intelligence and Soft Computing*, vol. 4, no. 1, pp. 1–28, 2014.
- [57] K. Deb and R. B. Agrawal, "Simulated binary crossover for continuous search space," *Complex systems*, vol. 9, no. 2, pp. 115–148, 1995.
- [58] W.-L. Loh, "On Latin hypercube sampling," *The Annals of Statistics*, vol. 24, no. 5, pp. 2058 – 2080, 1996.
- [59] D. P. Kingma and J. Ba, "Adam: A method for stochastic optimization," 2017. [Online]. Available: <https://arxiv.org/abs/1412.6980>
- [60] R. Yuriy, L. Viatcheslav, and B. Borys, "A real-world benchmark problem for global optimization," *Cybern. Inf. Technol.*, vol. 23, no. 3, p. 23–39, Sep. 2023.
- [61] X. Qiu, J.-X. Xu, Y. Xu, and K. C. Tan, "A new differential evolution algorithm for minimax optimization in robust design," *IEEE Trans. on Cybern.*, vol. 48, no. 5, pp. 1355–1368, 2018.
- [62] F. Zhang, *The Schur complement and its applications*. Springer Science & Business Media, 2006, vol. 4.